IADIS International Journal on Computer Science and Information Systems
Vol. 7, No.1, pp. 18-31
ISSN: 1646-3692

POINT-BASED SIMILARITY ESTIMATION BETWEEN 2.5D VISUAL HULLS AND 3D OBJECTS

Konstantinos Moustakas. *Electrical and Computer Engineering Department, University of Patras, 26504, Rio-Patras, Greece*

Georgios Stavropoulos. *Centre for Research and Technology Hellas - Informatics and Telematics Institute, 6th km Charilaou-Thermi Road P.O.Box 60361, 57001, Thermi-Thessaloniki, Greece.*

Dimitrios Tzovaras. *Centre for Research and Technology Hellas - Informatics and Telematics Institute, 6th km Charilaou-Thermi Road P.O.Box 60361, 57001, Thermi-Thessaloniki, Greece.*

ABSTRACT

This paper presents a novel framework for point-based similarity estimation between 3D objects and 2.5D visual hulls. Initially, the protrusion map is estimated for both the visual hull that is generated by a range image and the 3D model that is followed by the extraction of the salient features that correspond to the highly protruding areas of the objects. Then, based on the concept that for a 3D object and a corresponding query range image, there should be a virtual camera with such intrinsic and extrinsic parameters that would generate an optimum range image, in terms of minimizing an error function that takes into account the visual hull and the salient features of the objects, when compared to other parameter sets or other target 3D models, matching is performed via estimating dissimilarity within the range image and salient feature space. Experimental results illustrate the efficiency of the proposed approach in benchmark datasets.

KEYWORDS

Range image, 3D object, salient features.

1. INTRODUCTION

The problem of full 3D object similarity estimation, registration, search and retrieval has been successfully addressed by many researchers in the past, while excellent and extensive surveys can be found in (Tangelder, 2008) and (Bustos, 2005). Partial 3D matching is a special case of 3D object matching that involves finding correspondences on parts of 3D models. One of the most challenging problems in partial matching, is finding correspondences between 3D

objects, when the information describing the objects is not complete (for example when only a view of an object or a range map of the object is available). The wide availability of range scanners and 3D digitizers and the emergence of next generation technologies in 3D graphics and computational equipment has significantly increased the interest, especially for partial matching using range data as input. The present paper proposes a ”query by range data” 3D model search algorithm based on a novel partial matching method of salient points of the range image and the 3D model.

1.1 Related Work

Many researchers worldwide are currently developing 3D model recognition schemes. A number of approaches exist in which 3D models are compared by means of measures of similarity of their 2D views (Loffler, 2000), (Cyr, 2001). More direct 3D model search methods focus on registration, recognition, and pairwise matching of surface meshes (Zhang, 1999), (Mori, 2001), (Johnson 1999). Unfortunately, these methods usually require a computational costly search to find pairwise correspondences during matching.

Significant work has also been done in matching 3D models using geometric characteristics, where initial configurations are derived from conceptual knowledge about the setup of the acquisition of the 3D scene (Blais, 1995) or found automatically by extracting features such as curvature or edges (Chua, 2002). When correspondences between the two objects to be matched are unknown, the registration problem, which in general is not well posed, may approximately be solved by the iterative closest point (ICP) algorithm (Besl 1992). In the absence of a priori knowledge or robust features, the ICP algorithm starts with one unique or, preferably, multiple different initial configurations (Hugli, 1995). In (Hugli, 1997), a framework is presented for analyzing the subspace of the complete configuration space so as to force the ICP algorithm to converge to the global minimum. The method is evaluated experimentally for a number of real 3D objects.

Focusing on the problem of recognizing a 3D object when only a part of its shape is available as query few approaches have been presented in the past. Reeb Graphs are topological and skeletal structures that are used as a search key that represents the features of a 3D shape (Hilaga, 2001), (Bespalov, 2003). In (Biasotti, 2003) Reeb graphs that are obtained by using different quotient functions are obtained and highlight how their choice determines the final matching result. Other commonly used methods for 3D matching, that also support partial matching use *Local features* as described in (Gal, 2006) and (Shilane, 2007), while salient features have recently demonstrated increased robustness to noise and occlusions (Stavropoulos, 2010). Finally, partial matching, can be also achieved with the use of *model graphs* (Cicirello, 2001), (El-Mehalawi, 2003) or point-based approaches (Ruggeri, 2010), (Stavropoulos, 2010). In (Macrini, 2002), utilizing shock graph matching, indexing using topological signature vectors is applied to implement view based similarity matching more efficiently. Moreover, in (Chen, 2003) the light field descriptor is presented that is based on the concept that if two objects correspond, then they should also correspond from every viewpoint. A similar approach is presented in (Vranic, 2004), the so called ``depth buffer''. However, these approaches do not deal with partial matching. Germann et al. (Germann, 2007) initially precalculate a number of range images from different points of view. Shum et al. (Shum, 1996) map the surface curvature of 3D objects to the unit sphere with the use of a spherical coordinate system. By searching over a spherical rotation space, a distance between

two curvature distributions is computed and used as a measure for the similarity of two objects. Finally sketch-based approaches have also been developed for the quick sketch of a partial primitive shape to be used as query in 3D search system (Moustakas, 2006), (Moustakas, 2009).

1.2 Motivation

The aforementioned approaches have a few drawbacks. In many cases, they use a priori information for registering the partial view with the complete 3D model, while they do not utilize the saliency information of the 3D objects. In the proposed method, salient features are generated based on the protrusion maps of 3D models. The protrusion maps provide a stochastic saliency-based representation of the 3D models that is seen experimentally to efficiently encode object shape and exhibit robustness to noise and occlusion. The proposed scheme is experimentally seen to be robust and efficient in benchmark datasets.

2. 3D OBJECT REPRESENTATION

The identification of similar areas is computationally very expensive if matching is performed by comparing the query range image with another range image extracted from the 3D model. Therefore, a subset of features for the range image and the 3D model should eventually be used that should be easy to handle and representative for each object. In the present paper, salient features are used, that lie in general in the most protruding areas of a 3D surface.

The 3D models of most databases are in general in various scales. In order to be able to easily compare the similarities between a query range image and a set of models, the models should be normalized to a common scale. Since the spherical coordinate system is used in the current scheme, the best choice would be to normalize each model to the *unit sphere* before extracting the salient points of the 3D models. It should be noticed that the database models are normalized to a common scale so as to ease the implementation of the matching algorithm, even if the normalization is not a crucial process.

2.1 Protrusion Maps

The developed method for salient feature extraction that correspond to sharp locally protruding areas of the object's surface (Moustakas, 2007), (Lin, 2004) is based on Hoffman and Singh's theory of salience (Hoffman, 1997). A brief description of the method follows.

Initially, the dual graph *G=(V,E)* of the given triangulated surface is generated, where *V* and *E* are the dual vertices and edges. A dual vertex is the center of mass of a triangle and a dual edge links two adjacent triangles. The degree of protrusion for each dual vertex results from the following equation:

$$p(\mathbf{u}) = \sum_{i=1}^{N} g(\mathbf{u}, \mathbf{v}_i) \cdot area(\mathbf{v}_i) \qquad (1)$$

where N is the number of dual vertices in the entire surface, p(**u**) is the protrusion degree for the dual vertex **u**, g (**u**, $\mathbf{v_i}$) is the geodesic distance of **u** from dual vertex $\mathbf{v_i}$ and *area*($\mathbf{v_i}$) is the area of the triangle corresponding to $\mathbf{v_i}$.

2.2 Protruding Points

Using simple gradient based methods (i.e. steepest descent) all local maxima of the protrusion map p(**u**) are obtained. Geodesic windows are then applied and only the global maxima inside the window are considered as salient. A geodesic window, *GW*, centered at the dual vertex **u** is defined as follows:

$$GW_{\mathbf{u}} = \left\{ \mathbf{v} \mid \forall \mathbf{v} \in V, g\left(\mathbf{u}, \mathbf{v}\right) < \varepsilon \right\} \quad (2)$$

where ε defines the window size. Consider now the generalization $GGW_{\mathbf{u}}$ of the geodesic window $GW_{\mathbf{u}}$ that refers to the union of all geodesic windows defined on the dual mesh that include **u**. The generalized geodesic window is defined as follows:

$$GGW_{\mathbf{u}} = \bigcup GW_{\mathbf{a}} \mid \mathbf{u} \in GW_{\mathbf{a}}, \quad \forall \mathbf{a} \in V \qquad (3)$$

Assuming the set of salient features *S* that is a subset of the set of dual vertices *V*, then a dual vertex **s** is characterized as protruding

$$\mathbf{s} \in S \subset V \qquad (4)$$

if and only if the following condition holds:

$$\exists GGW_{\mathbf{s}} \quad so\ that \quad p\left(\mathbf{s}\right) = \max\left(p\left(\mathbf{u}\right)\right), \forall \mathbf{u} \in GGW_{\mathbf{s}} \qquad (5)$$

2.3 Processing Visual Hulls

In order to extract salient features from the range image, a 3D visual hull should initially be formed. The surface is created using only a subset of the points of the image, so as to reduce the redundancy and size of the triangulated surface to be generated. Features on the range image are selected, as the ones with maximum minimal eigenvalue in a predefined window. After the 3D surface is formed, the salient features are extracted in the same way they are extracted for the 3D models. **Figure 1** illustrates the salient features extracted from the 3D model of an Ant and from its 2D projected range image.

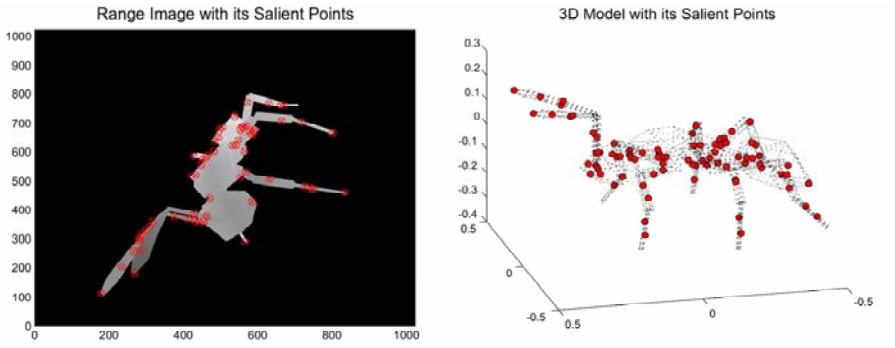

Figure 1. Ant model and the corresponding protruding points for a visual hull (left) and the full 3D model (right).

3. REGISTRATION AND MATCHING

The proposed framework is based on the assumption of a virtual camera, assumed to lie in the space of the examined 3D model. The search in the parameter space is performed for the set of camera parameters that capture a surface as similar as possible to the surface of the query range image.

3.1 Camera Model

Perspective projection using the standard pinhole camera model is adopted in the proposed method. The camera model consists of 10 parameters: resolution (r_w (width), r_h (height)), field of view (f_h (horizontal), f_v (vertical)), radius (ρ), longitude (φ), latitude (θ), roll (r) and z-axis offset (z_θ (yaw), z_φ (pitch)). From the aforementioned parameters, ρ, θ and φ define the position of the camera in space, while r, z_θ and z_φ define the orientation of the virtual camera. Finally, r_w, r_h, f_v and f_h define the internal structure of the camera.

Some of the camera parameters can be estimated prior to the matching process, in order to reduce the dimensionality of the parameter space and thus save computational power. The resolution of the camera is set equal to the resolution of the input image and the focal length can be explicitly estimated. Thus the parameters that need to be estimated are reduced to the following six (ρ, φ, θ, r, z_θ and z_φ)

3.2 Registration Using the Visual Hulls

The simplest way to perform matching between the query visual hull and the 3D object is to create a visual hull for every camera in space, for every possible set of parameters and compare it with the query visual hull. Although this method would be in the ideal case perfectly accurate, it is computationally unacceptable.

The most efficient way to search in the parameter space is by using *a spherical coordinate system* in order to describe the camera position. The spherical coordinate system ensures that

the virtual camera will "look" at the model which is placed in the center of the coordinate system.

Then, the range image of a particular view is generated using graphics hardware, in particular functions of OpenGL. After the range image is created, it is compared with the query range image by calculating the error for the current camera parameters using the following equation.

$$E\left(P_i, P_\theta\right) = \sum_{i,j=0}^{r_w, r_h} \left(I\left(i,j\right) - \hat{M}_{P_i, P_\theta}\left(i,j\right)\right)^2 \qquad (6)$$

where *I* corresponds to the query range image, while *M* refers to the rendered view of the 3D object for a given set of intrinsic and extrinsic virtual camera parameters (P_i, P_e). The set of camera parameters (P_i, P_e) that minimizes equation (6) is considered the best match. It should be noticed that the range image error function includes all the pixels that belong both to the query and the database object's image, only if the common area of both images is larger than a predefined threshold that is set to be 0.75 with respect to the size of the query object. Thus, if less than the 75% of the query object match with the target then this set of camera parameters is considered as non-matching set.

3.3 Registration using the Protruding Points

Even if exhaustive matching is very accurate, it is also computationally very expensive. A way to accelerate the matching process could be to use only a number of feature points of the range image and the 3D model. In the context of the proposed method, salient protruding points are used.

If the virtual camera described in the Section 3.1 exists and the query range image corresponds to the 3D model, then if a set of salient points is extracted from the query range image and another one from the surface that the virtual camera captures, then these two sets of points should also have corresponding subsets of features.

A set of salient points is extracted for the query range image, and another one for the 3D model. The later is transformed for each set of camera parameters (P_i, P_e), in order to be able to project the salient points on the virtual camera plane. These sets of points are used to calculate the similarity between the query range image and the 3D model.

The salient points extracted from the range image (I^S_i) are, in general, not identical to the ones extracted from the 3D model (M^S_j). In order to register the two sets of salient points, the salient points (M^S_j) of the 3D model are projected on the virtual camera plane thus creating a set of 2D salient points ($\hat{M}^S_j\left(P_i, P_j\right)$). Each of the projected salient points is registered with a salient point I^S_i, when the Euclidian distance between them V_k, is smaller than a threshold τ_v:

$$V_k\left(I^S_i, \hat{M}^S_j\left(P_i, P_e\right)\right) = \infty \quad if\ V_k > \tau_v \qquad (7)$$

and

$$V_k\left(I^S_i, \hat{M}^S_j\left(P_i, P_e\right)\right) = V_k \quad if\ V_k < \tau_v \qquad (8)$$

where τ_v is found empirically to be 3% of the resolution of the image.

Another constraint taken into account is that depth difference between the salient points d_k should also be smaller than a threshold τ_d:

$$d_k\left(I_i^S, \hat{M}_j^S\left(P_i, P_e\right)\right) = \infty \quad if\ d_k > \tau_d \qquad (9)$$

and

$$d_k\left(I_i^S, \hat{M}_j^S\left(P_i, P_e\right)\right) = d_k \quad if\ d_k < \tau_d \qquad (10)$$

A protruding point from the range image is registered with one from the 3D model only if both constraints described in equations (7)-(10) are satisfied.

More specifically the distance function E_S used to calculate the difference between the two sets of salient points, takes into account the 2D distance of the projected salient points compared, as well as their depth difference:

$$E_S\left(P_i, P_e\right) = \frac{1}{N_S}\sum_{k=0}^{N_S}\left(d_k\left(I_i^S, \hat{M}_i^S\left(P_i, P_e\right)\right) + V_k\left(I_i^S, \hat{M}_i^S\left(P_i, P_e\right)\right)\right) \qquad (11)$$

where N_S is the number of the registered salient points.

As in the case of exhaustive matching, the set of camera parameters that minimizes the function E_S is considered as the best match. In most cases, the actual number of salient points registered is significantly lower than the ones extracted in the original 3D model and the query visual hull. Therefore, at least 10 salient points have to be registered, in order to achieve correspondence between the query range image and the surface that the virtual camera captures.

3.4 Hierarchical Search

Even if the use of salient points reduces the computational complexity of matching full range images, the matching procedure remains computationally expensive when exhaustively searching in the parameter space. In the proposed framework a hierarchical approach is developed that reduces the computational complexity by several orders of magnitude.

The hierarchical search algorithm builds initially a coarse sampling of the 6D parameter space and evaluates for each sample the error function as described in Section IV. The sample that produces the minimum error is considered as best match and then the algorithm proceeds to the second layer of the hierarchy. In this layer the error function is evaluated around the local neighborhood of the "winning" sample and the new sample that produces the minimum error is considered as best match for the second layer of the hierarchy. This procedure is repeated until the final layer of the hierarchy is reached that corresponds to the maximum accuracy as previously described.

For the first level of the hierarchy the whole range image is used. After that, the search is done around the sample that gave the smallest error, with the use of salient features. This is done repeatedly until satisfactory accuracy in the parameter space is achieved. In order to achieve even better accuracy, for the last 3 levels of the hierarchy, instead of matching using salient points, the whole range image is used. This way any noise intruded by the salient points, is omitted, thus achieving increased accuracy (about 15%).

3.5 Accuracy Analysis

An important issue of the proposed method and of hierarchical methods in general, is to avoid the convergence of the algorithm in a local minimum of the function to be minimized. This issue has been carefully addressed by selecting the proper error function (range error or salient error) and by sampling the parameter space in such a way so as to minimize the possibility of convergence in a local minimum.

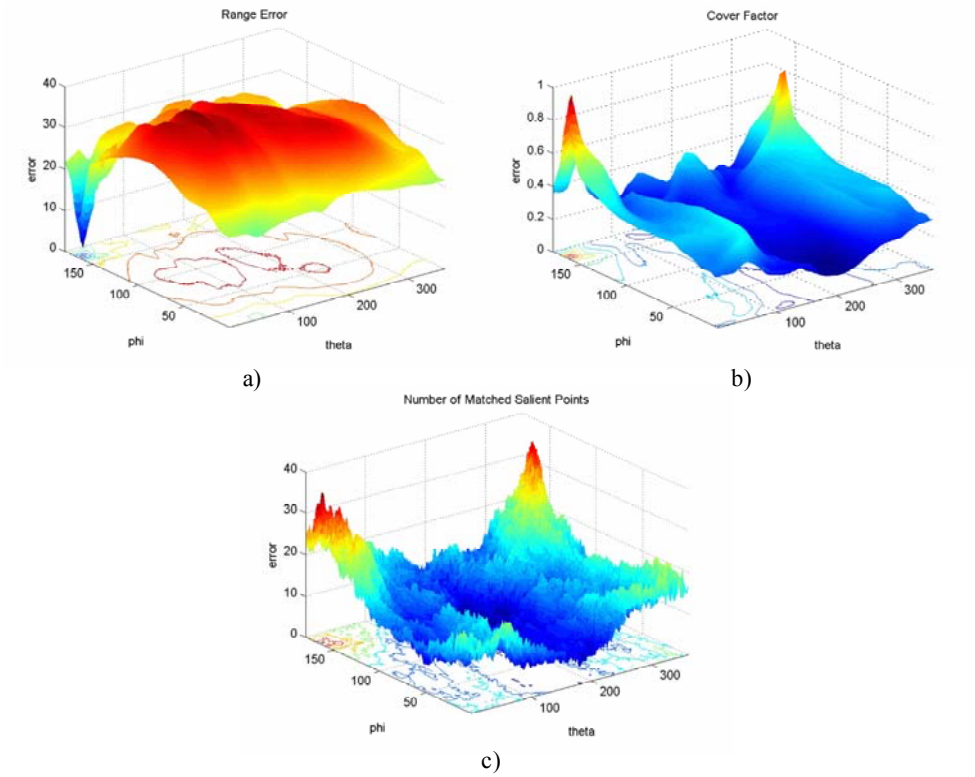

Figure 2. For an object of the database and for different values of θ and φ: a) Range error, b) cover factor rate (area of the joint support set for both the query and the target range image with respect to the query image area), c) number of salient pairs identified.

Figure 2 illustrates four diagrams that concern a single object of the database. In **Figure 2**a the range error is illustrated for all possible different values of θ and φ, while **Figure 2**b illustrates the cover factor rate that corresponds to the area of the joint support set for both the query and the target range image divided to the query image area. Notice that the global minimum can be clearly identified, while other local minima have much higher value. Moreover, the valley of the global minimum extends to more than 50^o for both the φ and θ parameters. This behavior is observed for all examined objects of the database and for the remaining parameters of the parameter space. Therefore, in the proposed algorithm, the initial sampling of the parameter space for the first level of the hierarchy is chosen to be in π/4

intervals. Coarser sampling would inhibit the performance of the algorithm, while denser sampling does not increase significantly the accuracy of the results, while slowing down the process.

Figure 2c depicts the number of salient pairs that are identified in the query and the target range image.

Figure 3 illustrates the same variables that appear in **Figure 2**, in the presence, however, of 20% occlusion. Notice that even if the number of salient pairs identified (**Figure 2**c) presents robustness to local minima and to occlusions as illustrated in

Figure 3c the range error and the cover factor demonstrate increased robustness. Therefore, despite the increased speed of the calculation of the salient error, in the first level of the hierarchy, where convergence is of high importance, the range error is used.

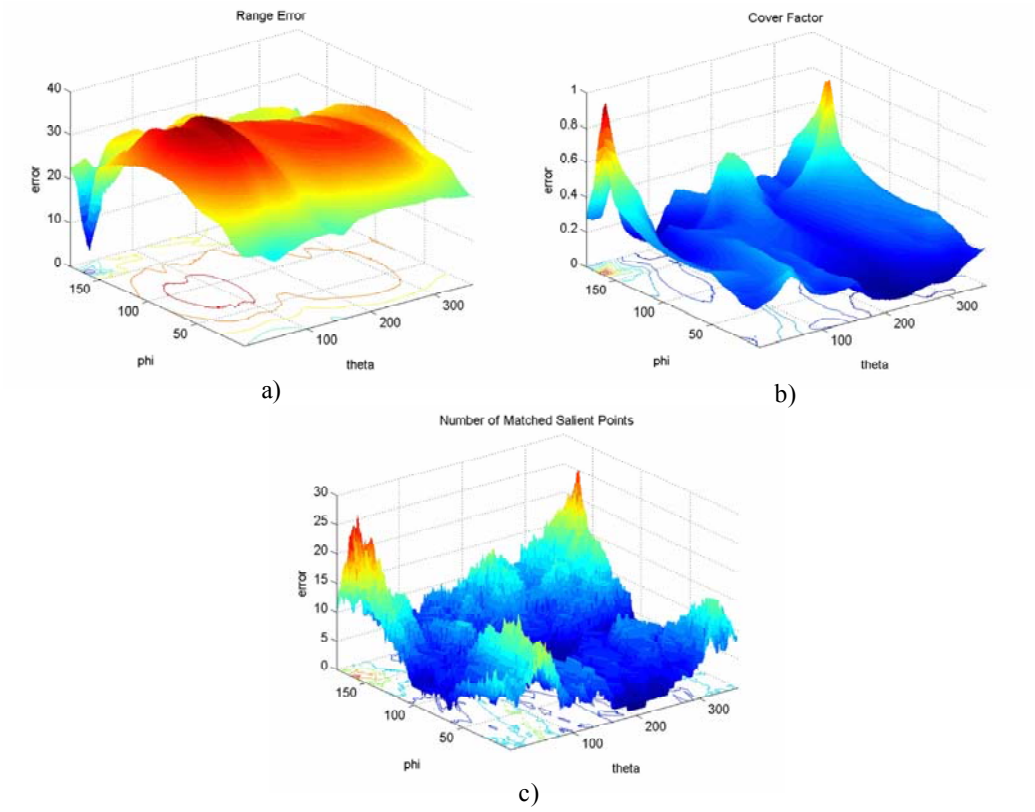

Figure 3. For an object of the database in the presence of occlusion (20%) and for different values of θ and φ: a) Range error, b) cover factor rate (area of the joint support set for both the query and the target range image with respect to the query image area), c) number of salient pairs identified.

4. EXPERIMETAL RESULTS

The proposed method was tested on the 3D model database of the Watertight model Track of Shape Retrieval Contest ’07. The database consists of 400 models organized in 20 categories. From the database, 400 range images where created from different views (one for each model), and entered as query in the matching algorithm. Each range image was compared with all the 3D models.

The following table describes the matching and retrieval efficiency of the proposed approach in terms of precision vs. recall, where precision is defined as the ratio of the relevant retrieved elements against the total number of the retrieved elements, and recall is the ratio of the relevant retrieved elements against the total relevant elements in the database. The first row of Table 1 refers to the precision of the proposed approach when the range image is used, while the second row refers to the precision, when 28dB Gaussian noise is added in the query range images.

Table 1. Precision of the proposed scheme for different recall values for clean – first row – and noisy – 28dB second row – range images.

Recall	**5%**	**10%**	**20%**	**30%**
Precision full	98%	89%	72%	59%
Precision noise	93%	82%	66%	52%

Moreover, Figure 4 illustrates the “precision vs. recall” curves for three different object classes. It is obvious that for classes with more representative shapes the matching scheme performs more efficiently.

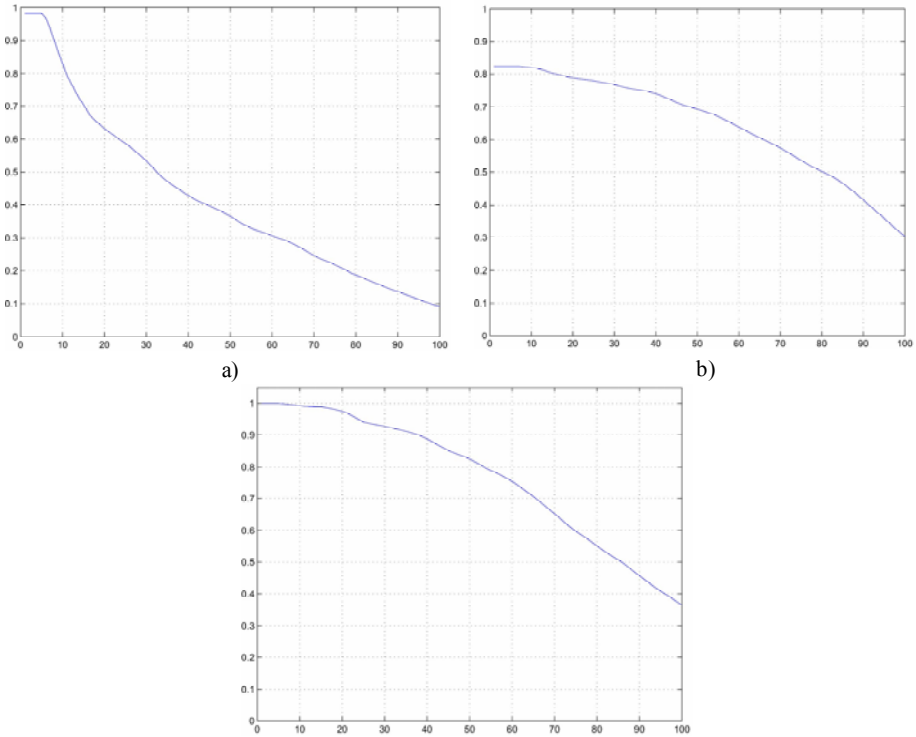

Figure 4. Precision vs. Recall curves for three different classes, namely a) animals, b) glasses, c) pliers.

Finally, Figure 5 illustrates examples of the query range images – first column of the table – and the retrieved results. Notice that in the second column the result stems from a different class (bird instead of airplane) exhibits however similar geometry. In the final row the input is a range image generated by a 3D scanner.

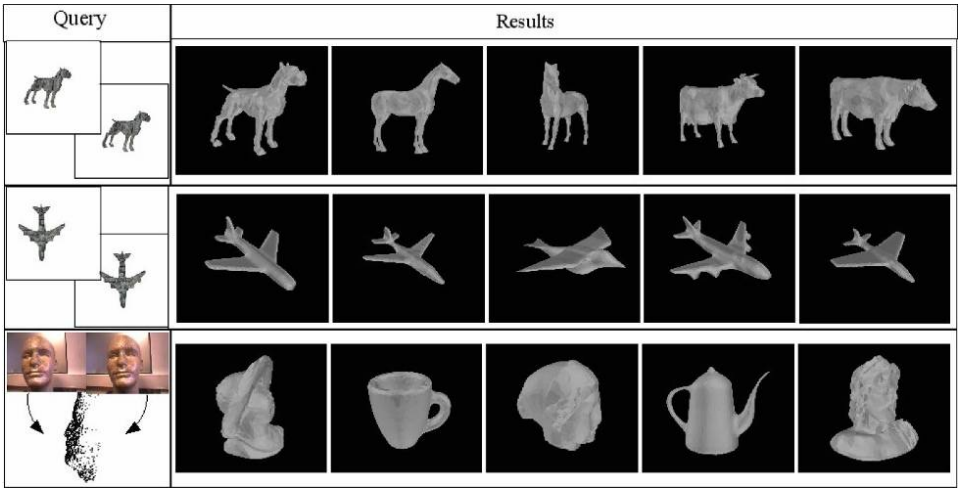

Figure 5. Example of query range images (first column) and the retrieved results.

5. CONCLUSION

In this paper a novel method for point-based similarity estimation between 2.5D visual hulls and 3D objects has been presented. The proposed approach introduces a description of 3D objects using salient protruding features that provide a compact description of the underlying geometry. Matching is performed via a hierarchical view-based approach so as to reduce the computational complexity of matching pipeline. The approach has been tested in a benchmark dataset and is also seen to be robust to occlusion. Moreover, the salient protruding features descriptor could be potentially extended to articulated or deformable models utilizing the manifold surface of the underlying geometries that forms our major future research direction in the field of 3D object retrieval through range image queries.

ACKNOWLEDGEMENT

This work was supported by the EU funded I-SEARCH IST STREP (FP7-248296)

REFERENCES

Bespalov D., et. al., 2003, “Scalespace Representation of 3D Models and Topological Matching,” In ACM Symposium on Solid Modeling ’03,pp.208-215.

Biasotti, S. et. al., 2003, 3D Shape Matching Through Topological Structures, DGCI, pp. 194-203.

Bustos, B. et. al., 2005, Feature-based similarity search in 3D object databases, ACM Computing Surveys, Vol. 37, No. 4, pp. 345-387.

Chen, D.Y. et. al., 2003, On visual similarity based 3D model retrieval, Computer Graphics Forum (EG 2003 Proceedings), Vol. 22, No. 3.

Cicirello V. and Regli W.C., 2001, "Machining Feature-based Comparisons of Mechanical Parts," SMI 2001, pp.176-185.

El-Mehalawi M. and Miller R.A., 2003, "A Database System of Mechanical Components Based on Geometric and Topological Similarity. part i: Representation," vol.31, no.1, Journal of Computer-Aided Design, pp.83-94,, January 2003.

Gal, R. and Cohen-Or, D., 2006, Salient geometric features for partial shape matching and similarity, ACM Transactions on Graphics, Vol. 25, No. 1, pp. 130-150.

Germann, M. et. al., 2007, Automatic Pose Estimation for Range Images on the GPU, Proc. 3D Digital Imaging and Modeling, 3DIM '07, pp. 81-90.

Hilaga M., et. al, 2001, "Topology Matching for Fully Automatic Similarity Estimation of 3D Shapes," In SIGGRAPH 2001, pp.203-212.

Hoffman D.D. and Singh M., 1997, "Salience of Visual Parts," Cognition, vol. 63, pp. 29-78.

Lin M., et. al., 2004, "Visual Salience-Guided Mesh Decomposition," Proc. IEEE Int'l Workshop Multimedia Signal Processing (MMSP).

Macrini D., et. al., 2002, "Viewbased 3-D object recognition using shock graphs," International Conference on Pattern Recognition (ICPR '02).

Moustakas K., et. al., 2006, "MASTERPIECE: Physical Interaction and 3D content-based search in VR Applications", IEEE Multimedia, vol. 13, no. 3, pp. 92-100.

Moustakas K., et. al., 2007, "SQ-Map: Efficient Layered Collision Detection and Haptic Rendering", IEEE Transactions on Visualization and Computer Graphics, vol. 13, no. 1, pp. 80 - 93

Moustakas K., et. al., 2009, "3D content-based search using sketches", Springer International Journal on Personal and Ubiquitous Computing, vol.13, no.1, pp. 59-67.

Stavropoulos G. et al. 2010, "3D Model Search and Retrieval from Range Images using Salient Features", IEEE Transactions on Multimedia, vol. 12, no.7, pp. 692-704, November 2010.

Ruggeri M., et. al., 2010, "Spectral-driven isometry-invariant matching of 3D shapes", International Journal of Computer Vision, Vol. 89, Numbers 2-3.

Shilane P., and Funkhouser T., 2007, "Distinctive Regions of 3D Surfaces," ACM Transactions on Graphics, vol. 26, no. 2, Article 7.

Shum, H.Y. et. al., 1996, On 3D Shape Similarity, Proc. IEEE Computer Vision and Pattern Recognition, pp. 526-531.

Stavropoulos G., et. al., 2010, "3D Model Search and Retrieval from Range Images using Salient Features", IEEE Transactions on Multimedia, vol. 12, no.7, pp. 692-704.

Tangelder, J.W.H. and Veltkamp, R.C., 2008. A survey of content based 3D shape retrieval methods. *In Multimedia Tools and Applications*, Vol. 39, No. 3, pp 441-471.

Vranic, D., 2004, 3D model retrieval, Ph.D. thesis, University of Leipzig, Germany.

Loffler J., 2000, "Content-based retrieval of 3d models in distributed web databases by visual shape information", In Proc. of Int. Conf. on Information Visualisation (IV2000), 2000.

Cyr C.M. and Kimia B., 2001, "3d object recognition using shape similiarity-based aspect graph", In Proc. of Int. Conf. on Computer Vision (ICCV2001), pages 254–261, 2001.

Zhang D. and Hebert. M., 1999, "Harmonic maps and their applications in surface matching", In Proc. of IEEE Conf. on Computer Vision and Pattern Recognition (CVPR99), 1999.

Mori G., Belongie S., and Malik J., 2001, "Shape contexts enable efficient retrieval of similar shapes", In Proc. of IEEE Conf. On Computer Vision and Pattern Recognition (CVPR2001), 2001.

Johnson A. E. and Hebert M., 1999, "Using spinimages for efficient multiple model recognition in cluttered 3-d scenes", IEEE Trans. on Pattern Analysis and Machine Intelligence (PAMI), 21(5):433–449, 1999.

Blais G. and Levine M., 1995, “Registering multiview range data to create 3d computer objects” IEEE Trans. on Pattern Analysis and Machine Intelligence (PAMI), 17(8):820–824, 1995.

Chua C.S. and Jarvis R., 2002, “3d free-form surface registration and object recognition”, In Proc. of Int. Journal of Computer Vision.

Besl B. J. and McKay N. D., 1992, “A method for registration of 3-d shapes”, IEEE Trans. On Pattern Analysis and Machine Intelligence (PAMI), 14(2):239–256, 1992.

Hugli H., Schutz C., and Semitekos D., 1995, “Geometric matching for free-form 3d object recognition”, In ACCV, Singapore, pages 819–823, 1995.

Hugli H. and Schutz C., 1997, “Geometric matching of 3d objects: Assessing the range of successful configurations”, In Proc. of Int Conf. of Recent Advances in 3-D Digital Imaging and Modeling, Ottawa, Ontario, Canada, May 1997.